Optical Materials 75 (2018) 821–826

Contents lists available at ScienceDirect

Optical Materials

journal homepage: www.elsevier.com/locate/optmat

Growth and spectroscopic properties of Sm^{3+}:$KY(WO_4)_2$ crystal

M.P. Demesh [a, *], O.P. Dernovich [a], N.V. Gusakova [a], A.S. Yasukevich [a], A.A. Kornienko [b], E.B. Dunina [b], L.A. Fomicheva [c], A.A. Pavlyuk [d], N.V. Kuleshov [a]

[a] Center for Optical Materials and Technologies, Belarusian National Technical University, 65 Nezalezhnasti Ave., Minsk, 220013, Belarus
[b] Vitebsk State Technological University, 72 Moskovskaya Ave., Vitebsk, 210035, Belarus
[c] Belarusian State University of Informatics and Radioelectronics, 6 Brovki Str., Minsk, 220013, Belarus
[d] Institute of Inorganic Chemistry, Siberian Branch, Russian Academy of Sciences, 3 Acad. Lavrentiev Ave., Novosibirsk, 630090, Russia

ARTICLE INFO

Article history:
Received 8 November 2017
Received in revised form
28 November 2017
Accepted 1 December 2017
Available online 6 December 2017

Keywords:
Double tungstate
Samarium
Crystal growth
Absorption
Luminescence
Cross-relaxation

ABSTRACT

A Sm^{3+}:$KY(WO_4)_2$ crystal was grown by the modified Czochralski technique. Polarized absorption and fluorescence spectra, as well as a fluorescence decay curve, were recorded at room temperature. Radiative properties such as emission probabilities, branching ratios and radiative lifetimes were investigated within the framework of the Judd-Ofelt theory as well as the theory of *f-f* transition intensities which takes into account the influence of the excited configurations. Emission cross section spectra were determined. $^4G_{5/2}$ fluorescence decay was analyzed within the framework of the Inokuti-Hirayama model. The spectroscopic properties of Sm:KYW crystal were compared with those of other Sm^{3+}-doped materials.

1. Introduction

There is increasing interest in finding new solid state media emitting in the visible spectral range. Rare-earth ions with emission in the visible spectral range are attractive for solid state lasers (without any nonlinear frequency conversion) and different applications: medicine (photodynamic therapy [1]), biophotonics, spectroscopy, quantum optics (atom trapping, atomic clocks, sodium guide stars [2]), communication, color displays, high density optical data storage and replacement dye lasers. Sm^{3+}- doped materials could be promising for these applications due to its strong orange-yellow fluorescence. Spectroscopic properties have been evaluated for Sm-doped single crystals [3–12], glasses [13,14], ceramics [15] and phosphors [16]. These investigations have shown the Sm^{3+} as a promising ion for solid state optical materials. Moreover, laser oscillation in the Sm^{3+} doped $LiLuF_4$ and $SrAl_{12}O_{19}$ crystals was obtained successfully [17].

The family of potassium double tungstates α-$KRE(WO_4)_2$ (RE = Y and Ln) crystals activated by rare-earth ions is a well-known host for solid-state lasers [18]. The main advantage of these crystals as a laser media is relatively high values of absorption and emission cross sections of rare-earth dopants. Also, double tungstates can be doped with high concentration of active ions without significant fluorescence quenching because of relatively large distances between the dopants ions [19].

This paper is devoted to the comprehensive spectroscopic characterization of Sm^{3+}:$KY(WO_4)_2$ (Sm:KYW) as a potential optical material. Polarization dependent absorption and fluorescence spectra were recorded. The conventional Judd-Ofelt theory and theories which take into account the influence of excited configurations were applied to determine the radiative properties of Sm^{3+} ions. Fluorescence decay curve of the $^4G_{5/2}$ level was registered and the excited state relaxation dynamics was discussed.

2. Experimental details

Sm:KYW crystal was grown by the modified Czochralski technique at low temperature gradient (<1deg/cm) using the [010] – oriented seed crystal from the potassium ditungstate ($K_2W_2O_7$) flux [20]. The mass content of the Sm^{3+} ions in the KYW crystal was determined using an ICP spectrometer IRIS Intrepid HR Duo (Thermal Elemental) and was found to be 0.434 ± 0.004 wt%. The

* Corresponding author.
E-mail address: demesh87@gmail.com (M.P. Demesh).

https://doi.org/10.1016/j.optmat.2017.12.001
0925-3467/

samarium concentration was calculated to be $1.14 \cdot 10^{20}$ cm^{-3} using measured volumetric crystal density of 6.58 g/cm^3. The as-grown crystal (see Fig. 1) was clear and had a good optical quality.

KYW is a biaxial crystal, with a monoclinic structure (space group C_{2h}^6 $-2/m$, Z = 4). Unit cell parameters for crystallographic setting $I2/c$ are a = 8.05 Å, b = 10.35 Å, c = 7.54 Å, β = 94°. There are two possible crystallographic settings $C2/c$ and $I2/c$ for this space group, however, the last one better describes the crystal habit [18]. Optical properties of KYW crystal are different for directions along the optical indicatrix axes N_p, N_m, N_g. Principal axis N_p coincides with the crystallographic ***b*** axis ([010]). The other two ones lie in the ***a-c*** plane. The principal axis N_g is rotated at 19° anticlockwise from ***c*** crystallographic axis. Its orientation was determined using a polarizing microscope POLAM-L213-BE (LOMO).

Samarium ions substitute yttrium ions in the KYW crystal and occupy the C_2 local point symmetry positions. The ionic radius of Sm^{3+} ion (1.079 Å) is close to one of the Y^{3+} (1.019 Å) for eight-fold coordination [21]. The separation between Y-Y pairs affects the energy transfer between the dopant ions. For KYW crystal this distance in the YO_8 chain parallel to the [101] direction is 0.406(3) nm and between different chains is 0.604(2) nm [18].

For the spectroscopic investigations a sample of Sm:KYW crystal was cut parallel to principal optical plains. The absorption and luminescence spectra of the Sm:KYW crystal were measured at room temperature with light polarized parallel to the three principal optical indicatrix axes. The absorption spectra in polarized light were recorded by a CARY 5000 spectrophotometer with a spectral bandwidth (SBW) of 0.1 nm in the UV and visible ranges and 0.3 nm in the NIR spectral range.

Fluorescence spectra were recorded under an InGaN-laser diode excitation at 405 nm. The luminescence emission was collected by a wide-aperture lens and focused onto the entrance slit of a monochromator MDR-23 (SBW = 0.1 nm). The signal was detected with a Hamamatsu C5460-01 APD module connected to a SR830 Standford lock-in amplifier. A Glan-Taylor polarizer was used to separate light polarizations. A gray body light source with a color temperature of 2900 K was used to correct the measured spectra with respect to detector response, grating efficiency, and other optical elements.

The decay curve of the upper manifold ($^4G_{5/2}$) was registered under pulsed excitation at 480 nm by means of an optical parametric oscillator LOTIS TII LT-2214, which was pumped by a third harmonic of the flashlamp-pumped Q-switched Nd:YAG laser LOTIS TII LS-2137. The fluorescence emission at the wavelength of 649 nm was imaged by wide aperture lens onto the entrance slit of a monochromator MDR-12. The signal was detected by a fast Hamamatsu photodetector C5460 connected to an oscilloscope with a bandwidth of 500 MHz.

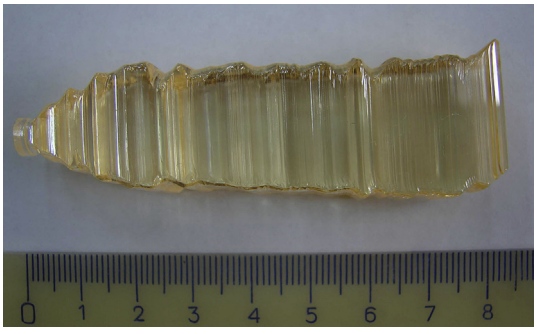

Fig. 1. Sm-doped KYW crystal boule.

3. Results and discussion

3.1. Absorption spectra

The polarized dependent absorption spectra of the Sm:KYW were recorded in the 350–570 nm and 970–3100 nm spectral ranges. The spectra were corrected for the Fresnel losses using the Sellmeier's coefficients for the KYW crystal [18]. The spectra of absorption cross section σ_{GSA} in the visible and NIR spectral ranges are shown in Fig. 2. The absorption bands within the $4f^5$ samarium configuration can be divided into two groups. The first one, appearing in the NIR region consists of quite intense lines which are assigned to the spin-allowed transitions from the ground state $^6H_{5/2}$ to the excited multiplets $^6H_{J'}$ and $^6F_{J'}$. Another group located in the UV and visible regions consists of a great number of closely spaced levels. Spin forbidden transitions occur between these levels and the ground state level. Hence the intensities of lines are weak, excepting spin allowed $^6H_{5/2} \rightarrow {}^6P_{J'}$ transitions. It should be noted, that identification of observed absorption bands in the UV–vis spectral range is difficult due to their strong levels overlapping. Assignments of the spectral lines for the excited states from the ground state were performed according to Ref. [22].

The absorption spectra of the Sm:KYW exhibits significant polarization dependence with dominant $E||N_m$ polarization. The strongest transition $^6H_{5/2} \rightarrow {}^6P_{3/2}$ has a peak value of absorption cross section of $9.2 \cdot 10^{-20}$ cm^2 at 404.6 nm for $E||N_m$ polarization. This value is larger than observed in Sm:NaGd$(MoO_4)_2$ [6], Sm:$GdVO_4$ [11], Sm:(Ca,Mg,Zr)GGG [12] Sm,Mg:SRA, [17].

3.2. Analysis of f-f transition intensities

To determine the transition intensities of Sm^{3+} ion in KYW crystal the Judd-Ofelt theory [23,24] was applied. The detailed description of the Judd-Ofelt analysis can be found in many papers but here we provide basics of this procedure. Measured absorption spectra were used to calculate experimental oscillator strengths f_{exp} between manifolds with quantum numbers J and J':

$$f_{\exp}(JJ') = \frac{mc^2}{\pi e^2 N_0 \bar{\lambda}^2} \int \overline{\alpha_{JJ'}(\lambda)} d\lambda, \quad (1)$$

where $\overline{\alpha_{JJ'}(\lambda)} = [\alpha_{Np}(\lambda) + \alpha_{Nm}(\lambda) + \alpha_{Ng}(\lambda)]/3$ is the polarization averaged absorption coefficient, $\bar{\lambda}$ is the weighted mean wavelength, N_0 is the concentration of Sm^{3+} ions. It should be noticed, that contribution of the magnetic dipole (MD) transitions ($\Delta J = 0, \pm 1$) from the ground state level to the several excited state levels was taken into account and, consequently, the electric dipole (ED) oscillator strengths $f_{\exp}^{ed}$ were obtained. The values of the double reduced-matrix elements $||U^{(t)}||$ were calculated from the intermediate coupling approximation using the free-ion parameters for samarium ion in glasses [25]. The values of experimental and calculated ED absorption oscillator strengths $f_{\exp}^{ed}$ and f_{JO}^{ed}, respectively, and the root mean square deviation are given in Table 1. Three phenomenological intensity parameters Ω_t were evaluated by the least-square fitting procedure and are presented in Table 2.

The influence of the excited configurations on the absorption and luminescence spectral characteristics in the case of Sm^{3+} ions may be significant [26]. It was shown [26], that applying the theory of *f-f* transition intensities, which takes into account the influence of $4f^{N-1}5d$ excited configuration, improves the agreement of the calculated results with the experimental data. Thus, to determine the radiative properties of Sm^{3+} ion in KYW crystal we applied the theory of *f-f* transition intensities for the system with the

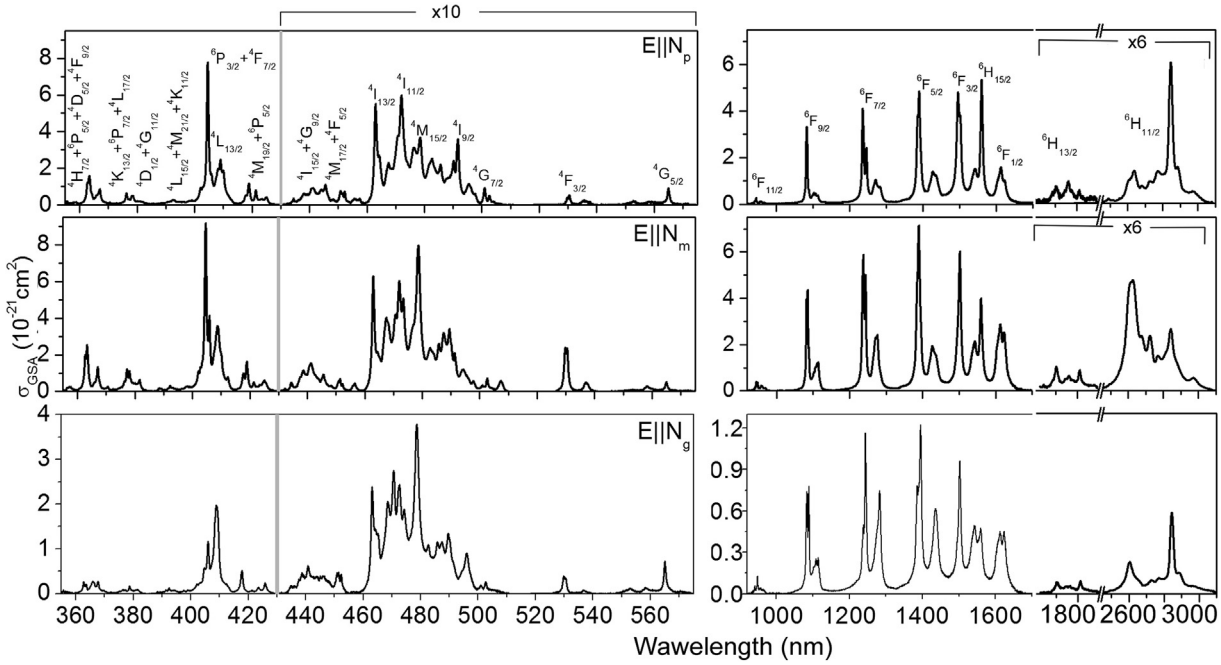

Fig. 2. Polarized ground absorption cross sections of Sm:KYW. Please note the different scales.

Table 1
Experimental (f^{ed}_{exp}) and calculated (f^{ed}) oscillator strength.

Transition $^6H_{5/2}$ →	Wavelength range (nm)	$\bar{\lambda}$ (nm)	f^{ed}_{exp}, 10^{-6}	f^{ed}_{JO}, 10^{-6}	f^{ed}_{MJO}, 10^{-6}	f^{ed}_{ICI}, 10^{-6}
$^6H_{11/2}$	2400–3100	2744	1.406	1.188	1.166	1.347
$^6H_{13/2}$	1780–2130	1957	0.292	0.347	0.342	0.389
$^6F_{1/2} + {}^6H_{15/2} + {}^6F_{3/2} + {}^6F_{5/2}$	1325–1700	1443	15.083	15.082	15.084	15.084
$^6F_{7/2}$	1180–1320	1251	6.5	6.509	6.509	6.504
$^6F_{9/2}$	1035–1145	1092	3.535	3.572	3.578	3.532
$^6F_{11/2}$	920–980	953	0.478	0.561	0.565	0.531
$^4G_{5/2}$	545–575	561	0.086	0.076	0.078	0.079
$^4F_{3/2}$	526–540	531	0.146	0.017	0.018	0.02
RMS deviation				$0.11\cdot10^{-6}$	$0.13\cdot10^{-6}$	$0.1\cdot10^{-6}$

Table 2
Intensity parameters (Ω_t) for Sm^{3+}-doped crystals.

Crystal	Ω_2 (10^{-20} cm^2)	Ω_4 (10^{-20} cm^2)	Ω_6 (10^{-20} cm^2)	Refs.
Sm:KYW (JO)	10.63	7.16	3.074	This work
Sm:KYW (MJO)	11.567	7.722 $\alpha = 0.018\cdot10^4$ cm	3.303	
Sm:KYW (ICI)	14 $R_2 = 0.052\cdot10^4$ cm	7.49 $R_4 = 0.016\cdot10^4$ cm	1.11 $R_6 = -0.467\cdot10^4$ cm	
$Sm:NaGd(MoO_4)_2$	8.65	4.4	1.96	[6]
$Sm:LiNbO_3$	2.11	4.5	1.45	[8]
$Sm:CaNb_2O_6$	8.02	5.37	1.45	[9]

intermediate configuration interaction [27] (denoted as the ICI approximation). The line strength of the ED transition from initial J manifold to some terminal J' manifold, in this case, can be evaluated by the formula:

$$S^{ed}_{calc}(JJ') = \sum_{t=2,4,6} \Omega_t \left[1 + 2R_t\left(E_J + E_{J'} - 2E^0_f\right)\right] \cdot \left|\left\langle 4f^n[SL]J \middle\| U^{(t)} \middle\| 4f^n[S'L']J' \right\rangle\right|^2, \quad (2)$$

here E_J and $E_{J'}$ are the energies of the combined multiplets, E^0_f is the average energy of $4f^N$ configuration and R_t are additional parameters related to the configuration interaction.

Additionally, we applied the modified Judd-Ofelt theory (MJO) [28]. In this case, only the excited configuration of the opposite parity makes a significant contribution, and the line strength can be obtained from the following equation:

$$S^{ed}_{calc}(JJ') = \sum_{t=2,4,6} \Omega_t \left[1 + 2\alpha\left(E_J + E_{J'} - 2E^0_f\right)\right] \cdot \left|\left\langle 4f^n[SL]J\right\| U^{(t)} \left\| 4f^n[S'L']J'\right\rangle\right|^2. \quad (3)$$

The values of the experimental and the calculated ED absorption oscillator strengths f^{ed}_{exp} and f^{ed}_{calc}, respectively, are given in Table 1.

The obtained intensity parameters Ω_t for Sm:KYW are listed in Table 2 and compared with ones for other samarium doped crystals. The high value of the parameter Ω_2 suggests the high degree of covalency of the bonds between rare earth ions and their ligands [29].

Obtained intensity parameters were used to calculate ED radiative transition probabilities A_{ed}. Several transitions from the upper $^4G_{5/2}$ level to the lower multiplets fulfill the selection rules for MD transitions. MD radiative transition probabilities A_{md} can be calculated separately and added to the ED transition probabilities. The total radiative transition probability can be expressed as [22]:

$$A_\Sigma(JJ') = \frac{64\pi^4 e^2}{3h(2J+1)\bar{\lambda}^3}\left[\frac{n(n^2+2)^2}{9}S_{ed} + n^3 S_{md}\right]. \quad (4)$$

The calculated luminescence branching ratios for $J' \rightarrow J$ transitions $\beta_{J'J} = A(J'J)/\sum A(J'J)$ and the radiative lifetime $\tau_{rad} = 1/\sum A(J'J)$ are presented in Table 3.

As can be seen from Table 3 there is no significant difference in the results obtained by using the three theories (JO, MJO and ICI approximation) for Sm:KYW crystal, in contrast with the Sm:$LiNbO_3$ crystal [26]. It indicates a small effect of the excited configurations on the absorption spectra in our case.

3.3. Fluorescence properties

Polarized fluorescence spectra of Sm:KYW in the range of 540–970 nm were recorded under excitation at 405 nm and corrected to the spectral response of the luminescence set-up. Overview of polarization averaged fluorescence spectrum is presented in Fig. 3. The observed emission bands are related to the radiative transitions from $^4G_{5/2}$ manifold to the lower lying levels. Manifold to manifold branching ratios for the transitions from the upper state the $^4G_{5/2}$ to the lower lying states are found from:

$$\beta_{J'J} = \frac{\int \lambda I_{J'J}(\lambda)d\lambda}{\sum_J \int \lambda I_{J'J}(\lambda)d\lambda} \quad (5)$$

here $I_{J'J}(\lambda)$ is the spectral density fluorescence power in arbitrary units. The experimental averaged values of $\beta_{J'J}$ over three polarizations with respect to calculated ones are presented in Table 4. It can be seen that measured and calculated values are in a good agreement. It is evident that almost 90% emitted energy is distributed in the visible spectral range. In the case of Sm:KYW, Sm:$NaGd(MoO_4)_2$ [6] and Sm:$CaNb_2O_6$ [7] almost the half of the emitted energy belongs to the $^4G_{5/2} \rightarrow {}^6H_{9/2}$ transition. But for the most of Sm^{3+}-doped materials, the transition is $^4G_{5/2} \rightarrow {}^6H_{7/2}$ has the highest intensity [2,5,7,8,10–17].

The stimulated emission (SE) cross sections σ_{SE} for the most intense transitions $^4G_{5/2} \rightarrow {}^6H_J$ (J = 5/2, 7/2, 9/2 and 11/2) were calculated by the Füchtbauer–Ladenburg formula [30]:

$$\sigma^{\alpha}_{SE}(\lambda) = \beta\frac{\lambda^5}{8\pi c n^2 \tau_{rad}}\frac{3I^{\alpha}(\lambda)}{\int\left[I^{Np}(\lambda) + I^{Nm}(\lambda) + I^{Ng}(\lambda)\right]\lambda d\lambda}, \quad (6)$$

here $I^{\alpha}(\lambda)$ is the spectral density of fluorescence power ($\alpha = N_m$, N_p and N_g polarizations), τ_{rad} is the radiative lifetime of the $^4G_{5/2}$ level, β is the branching ratio of the corresponding transition. The obtained SE-spectra are displayed in Fig. 4 for the wavelength range between 555 nm and 730 nm. The highest cross section was found

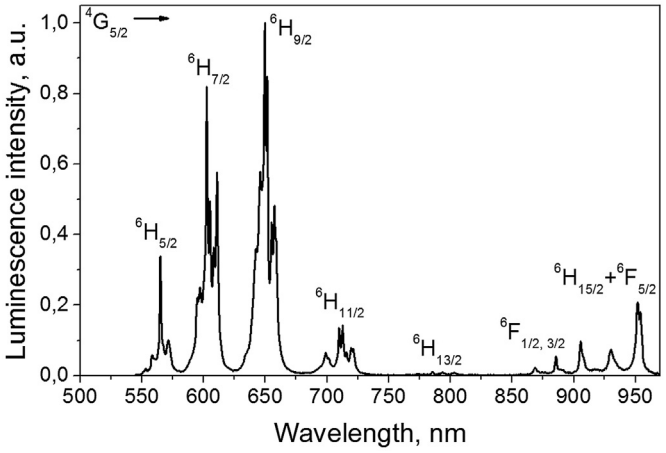

Fig. 3. Polarization averaged fluorescence spectra of Sm:KYW crystal.

Table 3
The calculated radiative probabilities (A_Σ), fluorescence branching ratios (β) in Sm:KYW crystal.

Transition $^4G_{5/2} \rightarrow$	$\bar{\lambda}$ (nm)	A_Σ (JO) (s^{-1})	A_Σ (MJO) (s^{-1})	A_Σ (ICI) (s-1)	β_{calc} (JO)	β_{calc} (MJO)	β_{calc} (ICI)
$^6H_{5/2}$	560	57.98	59.34	60.29	0.0048	0.0465	0.0471
$^6H_{7/2}$	595	331.13	344.29	300.96	0.2725	0.2697	0.2349
$^6H_{9/2}$	640	529.81	558.74	601.47	0.436	0.4377	0.4695
$^6H_{11/2}$	701	111.42	117.32	106.9	0.0917	0.0919	0.0834
$^6H_{13/2}$	772	15.17	16	8.5	0.0125	0.0125	0.0066
$^6F_{1/2}$	869	13.17	14.13	16.62	0.0108	0.011	0.013
$^6H_{15/2}$	877	27.44	28.68	61.74	0.0226	0.0225	0.0248
$^6F_{3/2}$	887	0.92	0.98	0.44	0.0008	0.0008	0.0004
$^6F_{5/2}$	923	99.34	103.32	121.9	0.0818	0.0833	0.0952
$^6F_{7/2}$	1007	13.09	13.89	13.3	0.0108	0.0109	0.0104
$^6F_{9/2}$	1131	14.69	15.91	18.4	0.0121	0.0125	0.0144
$^6F_{11/2}$	1343	0.89	0.92	0.59	0.0007	0.0008	0.0005
τ_{rad} (μs)					823	783	780

Table 4
Measured (β_{fJ}) and calculated (β_{calc}) branching ratios for the $^4G_{5/2}$ level in Sm:KYW crystal.

Transition $^4G_{5/2}$ →	Wavelength range, nm	β_{calc} (J-O)	β_{calc} (MJO)	β_{calc} (ICI)	β_{fJ}
$^6H_{5/2}$	545–580	4.8	4.6	4.7	5.8
$^6H_{7/2}$	580–625	27.3	27	23.5	26.2
$^6H_{9/2}$	625–678	43.6	43.8	46.9	43.9
$^6H_{11/2}$	685–737	9.2	9.2	8.3	8.1
$^6H_{13/2}$	765–810	1.2	1.3	0.7	0.8
$^6F_{1/2,\ 3/2,\ 5/2} + {}^6H_{15/2}$	865–970	11.6	11.8	13.3	15.2

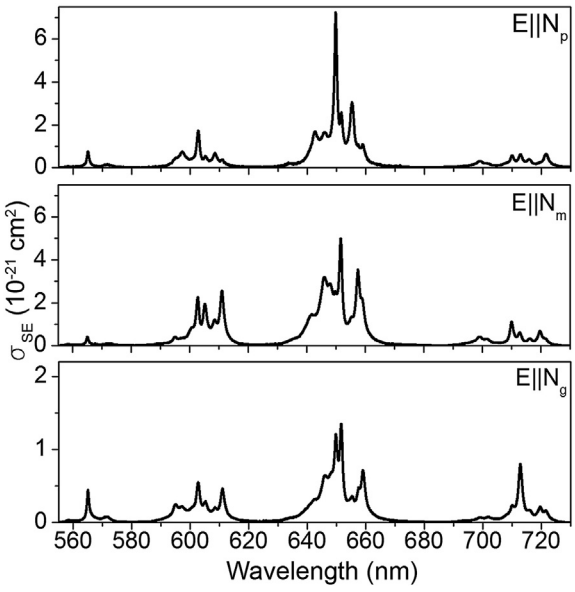

Fig. 4. Stimulated emission cross sections spectra of Sm:KYW crystal.

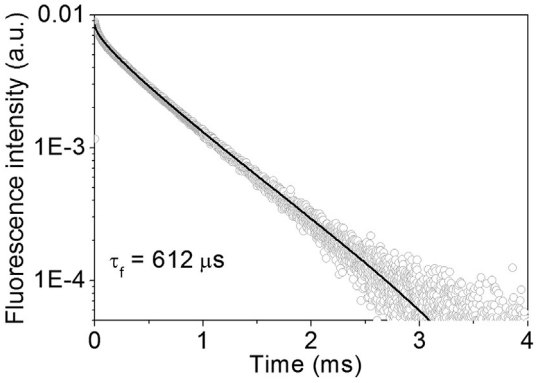

Fig. 5. Fluorescence decay curve of the $^4G_{5/2}$ multiplet of Sm:KYW crystal. The solid line represents fitted decay assuming dipole-dipole interactions.

to be $7.2\cdot10^{-21}$ cm^2 (λ = 649.7 nm) for N_p polarization and $5.2\cdot10^{-21}$ cm^2 (λ = 651.6 nm) for N_m polarization. In Table 5 we compare obtained in this study emission spectroscopic parameters of Sm:KYW crystal with ones of other Sm-doped materials.

3.4. Fluorescence dynamics

The fluorescence lifetime of the $^4G_{5/2}$ manifold was measured at 650 nm ($^4G_{5/2} \rightarrow {}^6H_{7/2}$ transition) under excitation at 480 nm. Fig. 5 shows a semilog plot of $^4G_{5/2}$ fluorescence decay curve, which has a non-exponential character due to the contribution of nonradiative cross-relaxation processes [31]. For Sm^{3+} ions the following resonance cross-relaxation mechanisms are possible: $^4G_{5/2} + {}^6F_{5/2} = {}^6H_{5/2} + {}^6F_{11/2}$ and $^4G_{5/2} + {}^6F_{11/2} = {}^6H_{5/2} + {}^6F_{5/2}$. Additionally, phonon-assisted cross-relaxation processes can occur. The decay curve can be fitted by the Inokuti-Hirayama (IH) model [32] for dipole–dipole energy transfer mechanism using the following expression:

$$I(t) = I_0 \exp\left(-t/\tau_0 - \gamma\sqrt{t}\right) \tag{7}$$

here τ_0 is an intrinsic lifetime of donor ions in the absence of an energy transfer. The parameter γ determines disordered static energy transfer and can be found by the following formula:

$$\gamma = \frac{4\pi^{3/2}}{3} N_0 R_0^3 \tag{8}$$

here R_0 is the critical transfer distance at which the nonradiative energy transfer rate becomes equal to the spontaneous emission rate [32]. The fitting procedure provides γ = 18.2 s$^{-1/2}$ and τ_0 = 0.78 ms. The comparable values of τ_{rad} and τ_0 show that there is no sufficient energy migration among the donors and we have dominantly the static disordered decay in this case [33]. The critical distance R_0 was derived as 0.84 nm and the average distance between samarium ions $R_{av} = (4\pi N_0/3)^{-1/3}$ was estimated to be 1.3 nm. Since the critical distance R_0 has a lower value than R_{av} it is expected that cross-relaxation processes which depopulate $^4G_{5/2}$ level in the Sm^{3+}(1.8 at%):KYW crystal are inefficient. The donor-acceptor energy transfer parameter $C_{DA} = R_0^6 \cdot \tau_0^{-1}$ was evaluated to be $4.6\cdot10^{-52}$ m^{6}s^{-1}.

Mean fluorescence lifetime τ_f was estimated to be 612 μs by the formula:

Table 5
Emission spectroscopic properties of some Sm^{3+}-doped crystals.

Crystal	N_{Sm}, (10^{20} cm^{-3})	λ_{peak} (nm)	σ_{SE} (10^{-21} cm^2)	τ_{meas} (μs)	τ_{rad} (μs)	η %	Refs.
$Sm:Gd_2SiO_5$	0.48	601	3.54	1.74	1.78	98	[5]
$Sm:NaGd(MoO_4)_2$	1.69	646	3.13	0.56	0.98	57	[6]
$Sm:SrAl_{12}O_{19}$	1.5	593	1.3	2.33	2.76	84	[7]
$Sm:LiNbO_3$	1.2	603	2.5	0.84	1.12	75	[8]
$Sm:CaNb_2O_6$	1.8	657	3	0.73	0.78	94	[9]
$Sm:LuLiF_4$	0.74	605	1.2	2.65	4.6	58	[10]
Sm:KYW	1.14	650	7.2	0.612	0.78	78	This work

$$\tau_f = \frac{\int tI(\lambda)d\lambda}{\int I(\lambda)d\lambda}. \quad (9)$$

The calculated radiative and experimentally determined emission lifetimes allow estimating the quantum yield of fluorescence which is about 78%. Table 5 lists the values of fluorescence lifetime and quantum efficiency η of the $^4G_{5/2}$ multiplet of several Sm^{3+}-doped crystals. The obtained results allow making a conclusion, that Sm(1.8 at%):KYW crystal has the quantum yield comparable to ones for other Sm-doped crystals.

4. Conclusions

We report on modified Czochralski growth and spectroscopic study of a 1.8 at% Sm^{3+}-doped $KY(WO_4)_2$ crystal. The spin allowed GSA-transition at 404.6 nm possesses a peak value of absorption cross sections of $9.2\cdot10^{-20}$ cm^2 for $E||N_m$ polarization. The highest stimulated emission cross sections of $7.2\cdot10^{-21}$ cm^2 and $5.2\cdot10^{-21}$ cm^2 were found in the orange spectral range at 649.7 nm (N_p-polarization) and 651.6 nm (N_m-polarization), respectively. To the best of our knowledge, Sm:KYW has the highest values of σ_{GSA} and σ_{SE} among known Sm-doped materials. The *f-f* transition intensities were calculated by applying the conventional and the modified Judd-Ofelt theories as well as the theory for the system with the intermediate configuration interaction. Based on these calculations the radiative lifetime of the upper state $^4G_{5/2}$ was derived to be about of 0.78 ms. The fluoresce lifetime and quantum efficiency of the $^4G_{5/2}$ multiplet were found to be 0.61 ms and 78%, respectively.

Acknowledgment

Authors greatly appreciate Dr. Rainer Bertram from the Institute for Crystal Growth (Berlin) for the measurement of the Sm^{3+} ions concentration.

References

[1] B.J. Chen, L.F. Shen, E.Y.B. Pun, H. Lin, Sm^{3+}-doped germanate glass channel waveguide as light source for minimally invasive photodynamic therapy surgery, Opt. Express 20 (2011) 879–889.
[2] L.A. Thompson, C.A. Gerdner, Experiments on laser guide stars at Mauna Kea Observatory or adaptive imaging in astronomy, Nature 328 (1987) 229–231.
[3] D. Pugh-Thomas, Spectroscopic properties and Judd–Ofelt analysis of BaY_2F_8:Sm^{3+}, J. Opt. Soc. Am. B 31 (2014) 1777–1785.
[4] J.B. Gruber, M.E. Hills, M.P. Nadler, M.R. Kokta, C.A. Morison, Absorption spectra and energy levels of Sm^{3+}:$Y_3Al_5O_{12}$, Chem. Phys. 113 (1987) 175–186.
[5] A. Strzęp, R. Lisiecki, P. Solarz, G. Dominiak-Dzik, W. Ryba-Romanowski, M. Berkowski, Optical spectra and excited state relaxation dynamics of Sm^{3+} in Gd_2SiO_5 single crystal, Appl. Phys. B 106 (2012) 85–93.
[6] J. Huang, J. Huang, Y. Lin, X. Gong, Y. Chen, Z. Luo, Y. Huang, Spectroscopic properties of Sm^{3+}-doped $NaGd(MoO_4)_2$ crystal for visible laser application, J. Lumin. 187 (2017) 235–239.
[7] C. Gheorghe, L. Gheorghe, A. Achim, S. Hau, R.D. Avram, Optical properties of Sm^{3+} doped strontium hexaaluminate single crystals, J. Alloys Compd. 622 (2015) 296–302.
[8] G. Dominiak-Dzik, Sm^{3+}-doped $LiNbO_3$ crystal, optical properties and emission cross-sections, J. Alloys Compd. 391 (2005) 23–32.
[9] A. Strzęp, W. Ryba-Romanowski, R. Lisiecki, X. Xu, J. Xu, J. Di, Spectroscopic characterization of $CaNb_2O_6$ single crystal doped with samarium ions, J. Lumin. 151 (2004) 123–129.
[10] G.Q. Wang, X.H. Gong, Y.F. Lin, Y.J. Chen, J.H. Huang, Z.D. Luo, Y.D. Huang, Polarized spectral properties of Sm^{3+}:$LiLuF_4$ crystal for visible laser application, Opt. Mater. 37 (2014) 229–234.
[11] X. He, L. Zhang, G. Chen, Y. Hang, Crystal growth and spectral properties of Sm:GdVO, J. Alloys Compd. 467 (2009) 366–369.
[12] W. Zhou, Q. Zhang, J. Xiao, J. Luo, W. Liu, H. Jiang, S. Yin, Sm^{3+}-doped (Ca,Mg,Zr)GGG crystal: a potential reddish-orange laser crystal, J. Alloys Compd. 491 (2010) 618–622.
[13] R. Vijaya, V. Venkatramu, P. Babu, C.K. Jayasankara, U.R. Rodríguez-Mendoza, V. Lavín, Spectroscopic properties of Sm^{3+} ions in phosphate and fluorophosphate glasses, J. Non-Cryst. Solids 365 (2013) 85–92.
[14] Sk. Mahamuda, K. Swapna, M. Venkateswarlu, A.S. Rao, S. Shakya, G.V. Prakash, Spectral characterizations of Sm^{3+} ions doped Oxy-fluoroborate glasses for visible orange luminescent applications, J. Lumin. 154 (2014) 410–424.
[15] C. Gheorghe, A. Lupei, F.M. Voicu, C. Tiseanu, Emission properties and site occupation of Sm^{3+} ion doped Lu_2O_3 translucent ceramics, J. Alloys Compd. 588 (2014) 388–393.
[16] Yu-C. Li, Yen-H. Chang, Yu-F. Lin, Yee-S. Chang, Yi-J. Lin, Synthesis and luminescent properties of Ln^{3+} (Eu^{3+}, Sm^{3+}, Dy^{3+})-doped lanthanum aluminum germanate $LaAlGe_2O_7$ phosphors, J. Alloys Compd. 439 (2007) 367–375.
[17] D.-T. Marzahl, P.W. Metz, C. Kränkel, G. Huber, Spectroscopy and laser operation of Sm^{3+}-doped lithium lutetium tetrafluoride ($LiLuF_4$) and strontium hexaaluminate ($SrAl_{12}O_{19}$), Opt. Express 23 (2015) 21118–21127.
[18] A.A. Kaminskii, A.F. Konstantinova, V.P. Orekhova, A.V. Butashin, R.F. Klevtsova, A.A. Pavlyuk, Optical and nonlinear laser properties of the $\chi^{(3)}$-active monoclinic α-$KY(WO_4)_2$ crystals, Cryst. Rep. 46 (2001) 665–672.
[19] P. Klopp, U. Griebner, V. Petrov, X. Mateos, M.A. Bursukova, M.C. Pujol, R. Sole, J. Gavalda, M. Aguilo, F. Güell, J. Massons, T. Kirilov, F. Diaz, Laser operation of the new stoichiometric crystal $KYb(WO_4)_2$, Appl. Phys. B 74 (2002) 185–189.
[20] A.A. Pavlyuk, Ya.V. Vasiliev, L.Yu. Kharchenko, F.A. Kuznetsov, Low thermal gradient technique and method for large oxide crystals growth from melt and flux, Proc. Asia Pac. Soc. Adv. Mater. (1993) 164–171. APSAM-92, Shanghai, China.
[21] R.D. Shannon, Revised effective ionic radii and systematic studies of interatomic distances in halides and chalcogenides, Acta Crystallogr. Sect. A 32 (1976) 751–767.
[22] W.T. Carnall, H. Crosswhite, H.M. Crosswhite, Energy Level Structure and Transition Probabilities in the Spectra of the Trivalent Lanthanides in LaF3 – Annual Report, Argonne National Laboratory, 1975.
[23] B.R. Judd, Optical absorption intensities of rare-earth ions, Phys. Rev. 127 (1962) 750–761.
[24] G.S. Ofelt, Intensities of crystal spectra of rare-earth ions, J. Phys. Chem. 37 (1962) 511–520.
[25] C.K. Jayasankar, E. Rukmini, Optical properties of Sm^{3+} ions in zinc and alkali zinc borosulphate glasses, Opt. Mater. 8 (1997) 193–205.
[26] E.B. Dunina, A.A. Kornienko, Influence of excited configurations on the intensities of electric-dipole transitions of rare-earth ions, Opt. Spectrosc. 116 (2014) 706–711.
[27] A.A. Kornienko, A.A. Kaminskii, E.B. Dunina, Dependence of the line strength of *f-f* transitions on the manifold energy. II. Analysis of Pr^{3+} in $KPrP_4O_{12}$, Phys. Status Solidi B 157 (1990) 267–273.
[28] R.T. Genova, I.R. Martin, U.R. Rodriguez-Mendoza, F. Lahoz, A.D. Lozano-Gorrin, P. Nunez, J. Gonzalez-Platas, V. Lavin, Optical intensities of Pr^{3+} ions in transpatrent oxyfluoride glass and glass-ceramic. Applications of the standard and modified Judd-Ofelt theories, J. Alloys Compd. 380 (2004) 167–172.
[29] S.A. Davis, F.S. Richardson, Hypersensitivity in the absorption spectra of Erbium (III) complexes in aqueous solution, Inorg. Chem. 23 (1984) 184–189.
[30] S.A. Payne, L.L. Chase, L.K. Smith, W.L. Kway, W.F. Krupke, Infrared cross-section measurements for crystals doped with Er^{3+}, Tm^{3+}, and Ho^{3+}, IEEE J. Quant. Electron. 28 (1992) 2619–2630.
[31] A.G. Avanesov, T.T. Basiev, Yu.K. Voron'ko, B.I. Denker, G.C. Maksimova, V.A. Myzina, V.V. Osiko, V.S. Fedorov, Investigation of spatial distribution impurities solids by the method of kinetic luminescent spectroscopy, Sov. Phys. JETP 57 (1983) 596–604.
[32] M. Inokuti, F. Hirayama, Influence of energy transfer by the exchange mechanism on donor luminescence, J. Phys. Chem. 43 (1965) 1978–1989.
[33] Yu.K. Voronko, T.G. Mamedov, V.V. Osiko, A.M. Prokhorov, V.P. Sakun, I.A. Shcherbakov, Sov. Phys. JETP 44 (1976) 251–261.